SEMARAK ILMU PUBLISHING

Journal of Advanced Research in Applied Mechanics

Journal homepage:
https://semarakilmu.com.my/journals/index.php/appl_mech/index
ISSN: 2289-7895

Extended Blade Element Momentum Theory for the Design of Small-Scale Wind Turbines

Siti Amni Husna Roslan[1], Zainudin A. Rasid[1,*], Ahmad Kamal Ariffin[2]

[1] Malaysia-Japan Japan International Institute of Technology, Universiti Teknologi Malaysia, 54100 Kuala Lumpur, Malaysia
[2] Faculty of Engineering and Built Environment, Universiti Kebangsaan Malaysia, 43600 Selangor, Malaysia

ARTICLE INFO

Article history:
Received 13 November 2022
Received in revised form 5 January 2023
Accepted 27 January 2023
Available online 31 January 2023

Keywords:
Small scale wind turbine, blade element momentum theory, tip loss factor, axial induction factor

ABSTRACT

Blade element momentum theory (BEMT) has been widely used in the design of the small scale wind turbine (SSWT). However, the original BEMT has weaknesses in providing the final design values of the wind turbine blade partly due to inaccurate assumptions of infinite number of blades made in deriving the theory. As such, the theory has to be amended in certain areas to form the so called the extended BEMT. In this study, a SSWT blade is designed using the extended BEMT method considering 3 factors: tip loss, low thrust at high axial induction factor, a and high angle of attack in post-stall region where 5 a correction models applying also the tip loss correction factor have been compared to the original BEMT model. The SSWT rotor has a diameter of 3m. An airfoil, SG6043 known for its suitability for SSWTs is used in this study. Furthermore, the blade geometry prior to the conduct of the shape optimization process are calculated using polynomial obtained from experimental procedures. The effect of infinite number of blades can be seen here to change the axial induction factor, a especially at the tip of the blade and as a result increases the lift coefficient, C_L and overpredicts the overall power coefficient and power of the wind turbine. With the Prandtl's tip loss factor along with the a correction model, the corrected final values of aerodynamic performances have been determined.

1. Introduction

The environment issues have been one of the main priority of the world's today to work on especially involving green and sustainable energy [1], material [2-4] and manufacturing process [5]. With the increase in population and industries, wind energy has become an important source of green and sustainable energy in the last decades. While Denmark has set a record of more than 40% usage of wind energy [6], the USA has put a target of having 20% wind energy in 2030 [7]. The wind energy is aimed to replace carbon-based energies that destroyed the environment as they have served the world for so long [8-10]. Today, the wind energy is well sought not only on shores but also in urban areas and low wind speed regions such that the demands for the small scale wind turbine (SSWT) is fast increasing. With this, the simple but yet efficient method of designing the wind turbine

* *Corresponding author.*
E-mail address: arzainudin.kl@utm.my

https://doi.org/10.37934/aram.101.1.6275

(WT) blade using the element momentum theory (BEMT) has been commonly used. However, the method still needs corrections partly due to the assumptions applied in the theory do not represent real conditions. As such the so called extended BEMT is used here considering 3 corrections in the loss of power at blade tips, loss of thrust at high axial induction factor, a and the loss of energy especially at high angle of attack after the occurrence of stall [11-13]. Noted that designing a SSWT requires such considerations on the wind condition, airfoil design, blade design and the energy loss factor. As such, studies on the corrections made to the BEMT method is actually focussing on the fourth design consideration mentioned above i.e. the energy loss factor.

In a research on the aerodynamic performance of a SSWT using the BEMT [14], it was shown that at a mere wind speed of 3 m/s, the wind turbine can have power coefficient of 43%. However, to produce power amounted to 600 W, a household need for electrical consumption, the wind speed needed was 5m/s. In considering the high axial induction factor, Damirez and Augusto [15] compared the results of the basic BEMT with those of the correction formulations given in literatures. The study found that the correction proposed by Buhl gave the closest results compared to wind tunnel experimental data taken from the literature. Similar comparison was made by Oliveira et al.[11] on the BEMT performances on the HAWT related to lost factors. The results from experimental study on the MOD-0 turbine were used. It was found that the BEM method combined with Prandtl (tip and root loss), Wilson and Spera corrections (high values of the axial induction factor), and Viterna and Corrigan (high angle of attack), presents a good prediction of the performance of horizontal-axis turbines.

In this study, the BEMT analysis focussing on the loss factors in the design of a SSWT is conducted. The effects of the 3 corrections embedded in the extended BEMT equations on the aerodynamic performance of a SSWT are studied. The well-known airfoil for the SSWT, namely the SG6043is used in this study. Furthermore, the blade geometry is following the Anderson's experimental based polynomial equations for chord length and twist angle [16]. The study provides the overall aerodynamic performances of the WT along with the distributions of important parameters throughout the blade length.

2. Methodology

The specifications of the wind turbine are given in this section. Furthermore, several models of the extended BEMT method are discussed. Referring to Table 1, while the number of blade is 2, the rotor radius of the SSWT considered here is 1.5m. The tip speed ratio (TSR), λ changes from 1 to 8 which covers a suitable range for SSWTs [17].

Table 1
The wind turbines specifications

Airfoils	SG6043
Wind speed, *V*	3-13 m/s
Rotor radius, *R*	1.5 m
No. of blade, *B*	2
No. of element	15
Tips speed ratio, *λ*	1-12

2.1 The Airfoil

The airfoil and Reynold's number, Re determine the value of the important parameter of gliding ratio, L/D. In this study, the airfoil used is the SG6043 that is known to be superior for the SSWT

application [18, 19]. This airfoil is as illustrated in Figure 1. Using XFOIL codes, the plots of L/D against angle of attack, AOA at Re=500000 for several airfoils are given in Figure 2. It shows that the SG6043 profile provides the highest L/D of 65. The critical AOA is slightly higher that of the Eppler and BW3 profiles at $\alpha_{cr} = 5°$. However, the stall here is considered abrupt as the range of AOA at the vicinity of maximum L/D is rather smaller compare to that of NACA6412.

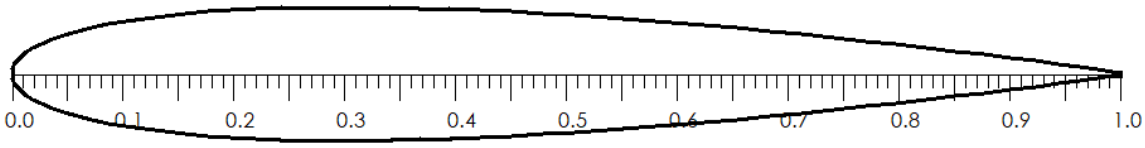

Fig. 1. The SG6043 airfoil

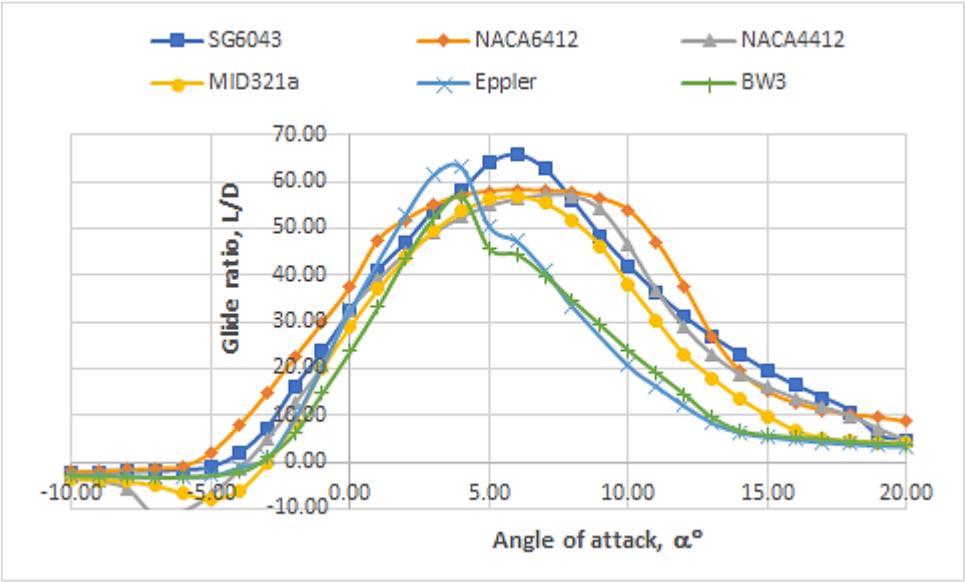

Fig. 2. The glide ratio vs angle of attack at Re = 500000

2.2 The BEMT Method

The BEMT analysis provides final design data for the blade's geometry, aerodynamic forces and aerodynamic performances of the wind turbine such as the power, P, power coefficient, C_P, thrust, F_a and torque, T_s. Referring to Table 2, the blade is divided into 15 elements where $Rn_i = r_i/R$ is the normalized position of the mid point of the i^{th} element. For each blade element, the chord length, c and the angle of twist, θ of the blade have been prepared according to the Anderson's polynomials that are based on the wind-tunnel experiment [16].

With the readily available values of c and θ and the assumed values of axial (a) and radial (a') induction factors, the flow angle, ϕ, AOA, relative wind speed, V_{rel} and Reynold's number, Re can be calculated [20]. Considering the AOA and Re as inputs, the values of lift coefficient, C_L and drag coefficient, C_D can be determined. The C_L and C_D for airfoils SG6043 have been determined for several specific Re ranging from Re=4000 to Re=600000 using the XFOIL codes that gives the values of the C_L and C_D over a range of AOAs. Thus, in this study, to get the values of C_L and C_D for different Re numbers, interpolations are conducted. With the values of the C_L and C_D, the new a and a' can be determined as in the following [20].

$$a = \frac{1}{\frac{4\sin^2\phi}{\sigma C_a}+1} \quad (1)$$

and

$$a' = \frac{1}{\frac{4\sin\phi\cos\phi}{\sigma C_t}+1} \quad (2)$$

With new a and a' values in this pure BEMT method, new iteration will be followed until the two induction factors converged.

Table 2
The radius, chord length and twist angle of the wind turbine

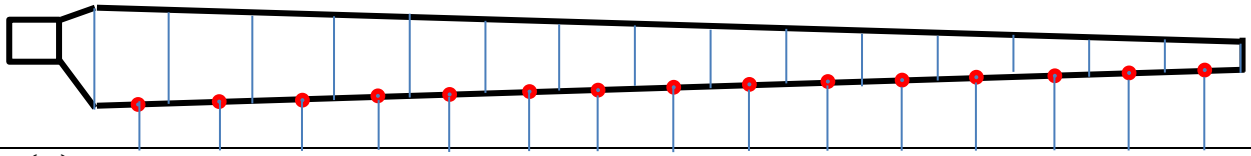

$Rn_i\ (m)$	0.13	0.19	0.25	0.31	0.37	0.43	0.49	0.55	0.61	0.67	0.73	0.79	0.85	0.91	0.97
c(cm)	24.73	16.77	11.28	7.61	5.23	3.69	2.65	1.87	1.21	0.63	0.17	- 0.26	- 0.68	- 1.11	- 1.53
$\theta(^\circ)$	0.17	0.14	0.11	0.09	0.08	0.07	0.06	0.05	0.05	0.05	0.04	0.04	0.04	0.03	0.03
Elem.	1	2	3	4	5	6	7	8	9	10	11	12	13	14	15

2.3 The Extended BEMT Method

The procedures explained above using the pure (nonextended) BEMT formula for a and a' can be containing errors and thus require corrections for more accurate results. The following discuss the 3 corrections in the applied extended BEMT method in this study.

2.3.1 Correction due to tip's loss

The first correction in the extended BEM is the application of the Prandtl's tip loss factor, F to correct the assumption of axisymmetric flow that model the helical vortex wake pattern as vortex sheets such that the rotor has an infinite number of blades. With tip loss, the difference exist between a two dimensional and a three-dimensional configuration of a turbine blade that is caused by the circulation flow driven by the pressure equalization which arises at the tip of the blade. In reality, the finite number of blades actually allows air flow to pass thru the blade, thus producing a non-uniformity on the flow leading into a variation of the induction factor around the rotor, then a loss of lift and hence a loss of power. With$F$, the gap between the Betz ideal flow and the real flow is getting smaller. F is defined as

$$F = \frac{2}{\pi}cos^{-1}\left[exp\left(-\frac{0.5B(r-R)}{rsin\phi}\right)\right] \quad (3)$$

As such, new axial and radial induction factors, a and a' respectively are

$$a = \frac{1}{\frac{4F\sin^2\phi}{\sigma C_a}+1} \quad (4)$$

and

$$a' = \frac{1}{\frac{4F\sin\phi\cos\phi}{\sigma C_t} - 1} \tag{5}$$

2.3.2 Correction due to high induction factor

The second correction of the BEMT is the effect of high axial induction factor, a that causes the reduction in the thrust force. This has made the pure BEMT method invalid as it contrasts to results from experimental procedures where the thrust force keep on increasing as a get higher [21]. The correction considered here are based on several proposed models in literature.

1) **Glauert's** [20, 21]
Defining the 2 parameters Y_1 and Y_2:

$$Y_1 = \frac{4Fsin^2\phi}{\sigma C_a} \tag{6}$$

$$Y_2 = \frac{4Fsin\phi cos\phi}{\sigma C_d} \tag{7}$$

The new a is then set to be:

$$a_n = \begin{cases} \frac{2+Y_1-\sqrt{4Y_1(1-F)+Y_1^2}}{2(1+FY_1)} & Y_1 \geq 2 \\ \frac{\left(2+Y_1c_t-\sqrt{\left((Y_1c_t+2)^2-4\left(1-\frac{1}{9}FY_1\right)\right)}\right)}{2} & Y_1 < 2 \end{cases} \tag{8a}$$

where

$$c_t = 1 - 2/3(\mathrm{F}) \tag{8b}$$

And the new radial induction factor,

$$a' = \frac{1}{\frac{(1-aF)Y_2}{(1-a)} - 1} \tag{9}$$

2) **Shen's [22]**
Define the following parameters,

$$g=\exp(-0.125*(N*\lambda-21)+0.1 \tag{10a}$$

$$f = 0.5(N)(1/r-1)/\sin(\phi) \tag{10b}$$

$$F_1 = 2/\pi * \cos^{-1}\left(e^{-g(f)}\right) \tag{10c}$$

For $C_a^r = F_1(C_a)$ and $C_t^r = F_1(C_t)$ and $Y_1 = \frac{4Fsin^2\phi}{\sigma C_a^r}$ and $Y_2 = \frac{4Fsin\phi cos\phi}{oC_t^r}$,

So,

$$aT = \frac{1}{2}(2 + Y_1 - \sqrt{(Y_1 * (4 * (1 - F) + Y_1))})(1 + F * Y_1)/2; \quad (11a)$$

$$a_n = \begin{cases} \frac{1}{K+1}, K = 4F(\sin^2(\phi)/\sigma C_a & aT \leq 1/32 \\ aT & aT > 1/32 \end{cases} \quad (11b)$$

3) **Wilson and Walker's [23]**
For $a > a_c$, where $a_c = 0.2$,

$$C_a = 4(a_c^2 + (1 - 2a_c)a)F \quad (12)$$

$$a = \frac{1}{2}\left[2 + K(1 - 2a_c) - \sqrt{(K(1 - 2a_c) + 2)^2 + 4(Ka_c^2 - 1)}\right] \quad (13)$$

Where

$$K = \frac{4Qsin^2\phi}{\sigma C_A} \quad (14)$$

4) **Buhl's [23]**

For $a > 0.4$,

$$a = \frac{\left(18\sigma C_a + 36F^2 sin^2\phi - 40Fsin^2\phi - 6\sqrt{(18F\sigma C_a sin^2\phi + 36F^4 sin^4\phi - 48F^3 sin^4\phi)}\right)}{2(9\sigma C_a - 50Fsin^2\phi + 36F^2 sin^2\phi} \quad (15)$$

2.3.3 Correction due to stall

The third correction of the BEMT is due to the occurrence of stall. This extension of the BEMT includes incorporating the effects of the flat plate region i.e. the post-stall region where the BEMT underestimates the rotor power when compared to experimental results. This is due to lacks of accurate values of C_L and C_D at off-design condition of post-stall region [24]. In this study, the values of C_L and C_D interpolated for post-stall region by Viterna and Corrigan by applying an empirical model will be used [25]:

For $\alpha_{\text{separation}} < \alpha < 90^{\text{o}}$:

$$C_L = \frac{C_{D,max}}{2}\sin 2\alpha + K_L\frac{\cos^2\alpha}{\sin\alpha} \quad (16)$$

$$C_D = C_{D,max}\sin^2\alpha + K_D\cos\alpha \quad (17)$$

where

$$K_L = \left(C_{L,s} - C_{d,max}\sin\alpha_s\cos\alpha_s\right)\frac{\text{Sin}\,\alpha_s}{\text{Cos}^2\alpha_s} \quad (18)$$

$$K_D = \frac{C_{D,s} - C_{D,max} \sin^2 \alpha}{\cos \alpha_s} \quad (19)$$

$C_{D,max}$ is the maximum drag coefficient for the completely separate region that is based on the aspect ratio, μ such as

$$\mu \leq 50: C_{D,max} = 1.11 + 0.018\mu \quad (20)$$

$$\mu > 50: C_{D,max} = 2.01 \quad (21)$$

where

$$\mu = \frac{R - r_{hub}}{c(r)} \quad (22)$$

For the range of 90° and 180° (+ve and -ve), the C_L and C_d can be taken as the flat plate/fully stalled region values [26, 27]:

For $90^o < \alpha < 180^o$:

$$C_L = C_{L,plat} = 2 \sin \alpha \cos \alpha \quad (23)$$

$$C_D = C_{D,plat} = 2 \sin^2 \alpha \quad (24)$$

The BEMT analysis here is conducted through a developed MATLAB's codes [28].

3. Results

In this section, the performances of the wind turbine in the forms of power coefficient, C_p, torque, T, power produced, P and thrust, F_a are deliberated under the effects of the three correction factors considered here. Prior to that, the behaviours of the aerodynamic parameters such as a and a' throughout the blade are discussed as well. Noted that the significant of the 3rd factor is there as the variation of the TSR will cause the increase of AOA to above critical angle, α_{cr} and such the importance of using the 3rd extended BEMT cannot be stressed more.

3.1 The Aerodynamic Parameter Behaviour Throughout the Blade

The study here is done at a specific wind speed, V=5m/s and TSR=7. The graphs of axial and radial induction factors against the blade position are given in Figures 3 (a) and (b), respectively. From Figure 3(a), it shows the reduction of a values moving toward the tip of the blade for all models under consideration except the BEMT with tip loss model. All four models show similar values of a up to the mid-range of the blade length. The concerned effect of tip loss can be clearly seen in the graph as it approaches the blade's tip. For the pure BEMT model where the Prandtl's tip loss factor, F is not considered, the infinite rigid blade has caused a to reduce greatly at the tip. However, considering the F in the BEMT with Prandtl's tip loss, the values of a can be seen to increase greatly. Considering also the a correction factors in the Glauert and Wilson-Walker models, the values of a are brought down to give moderate increases if compared to the pure BEMT model. Table 3 shows the different values of a at the mid-point of the las element at the blade's tip where the BEMT with tip loss effect

has moved up the a values by about 208% while the Gluert and the Wilson Walker models move closer back to the BEMT model by having about 107% and 139%, respectively.

Table 3
The difference between α of 4 different correction models

Model	BEMT	BEMT+ Tip Loss	Gluert	Wilson-Walker
α	0.084	0.259	0.174	0.201
% difference from α	0	208.33	107.1429	139.2857

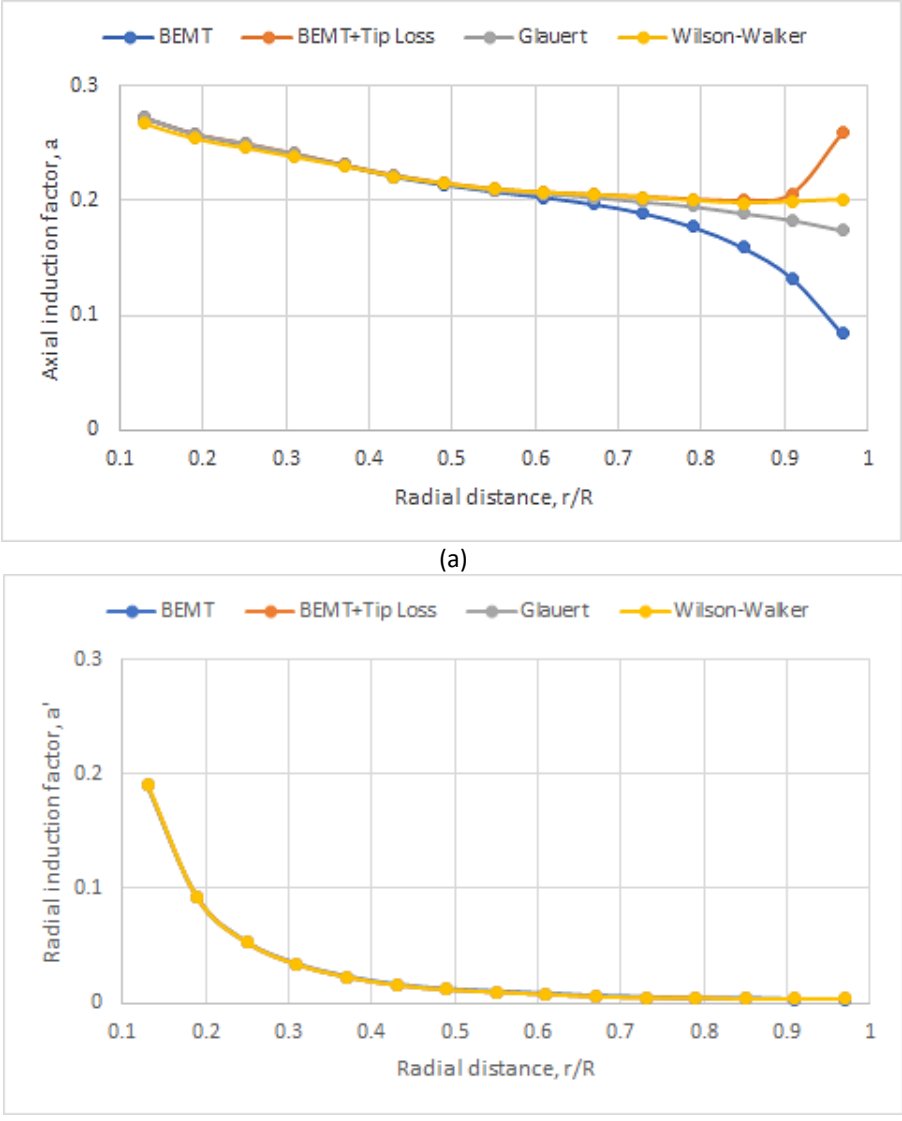

(a)

(b)

Fig. 3. The (a) axial and (b) radial inductions factors against radial positions of the blade

In contrast, as the effect of the tip loss and the a correction factor are mainly related the thrust of the blade, they can be seen to have no effect on the radial induction factor. The 3 models show equal plots of the a' vs r/R graphs moving from hub to tip position as shown in Figure 3 (b).

Without the non-uniformity of a for turbine with infinite number of rigid blades, the pure BEMT model gives an overpredicted coefficient of lift, C_L such as shown in Figure 4. While the effect is none at the first middle-half of the blade, the BEMT model gives the highest C_L of 1.283 at the blade's tip.

As expected, the addition of the tip loss factor decreases the C_L to 1.122 where the models of Glauert and Wilson-Walker can be seen to increase back the C_L to 1.2 and 1.173 respectively. Noted that the maximum value of C_L can be seen at about $R_n = \frac{r}{R} = 0.3$. With the behaviours of a and C in Figure 3(a) and 4, it can easily be expected that the pure BEMT theory will over-predict the thrust, power coefficient and power especially at the tip of the blade while the correction models of Glauert and Wilson-Walker will close the gap between the Glauert and the BEMT with tip loss model.

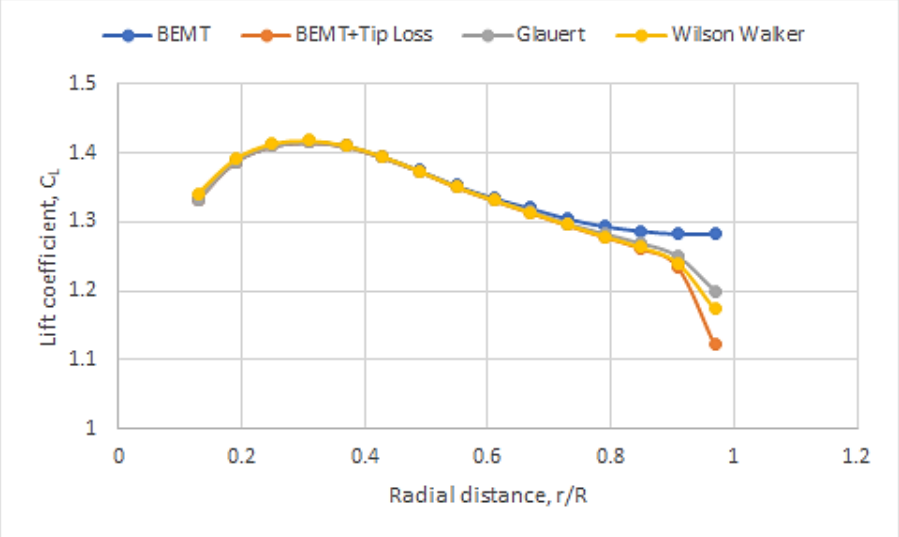

Fig. 4. The coefficients of lift, C_L against radial positions of the blade

The variations of two important parameters that determine the lift and drag coefficients of the airfoil and thus the aerodynamic performances of the wind turbine i.e., the AOA and Re throughout the blade radius for different TSR can be seen in Figure 5 and 6 respectively. This analysis is based on the Glauert's model. The AOAs can be seen to increase moving from the hub and after reaching a maximum value, AOAs will decrease as the curve moves toward the blade's tip. It is apparent also that as the TSR is increased, the applied AOA is decreased thought the blade. It shows that at low TSR, the blade has AOAs beyond the critical angle, α_{cr} for the airfoil SG6043 in this study. Thus, the need for interpolating values C_L and C_D can be seen here. In contrast, the Re seems to be decreased for small TSR and increased for higher TSR as the curves move toward the blade's tip. Also, as the TSR is increased, the Re is increasing as well.

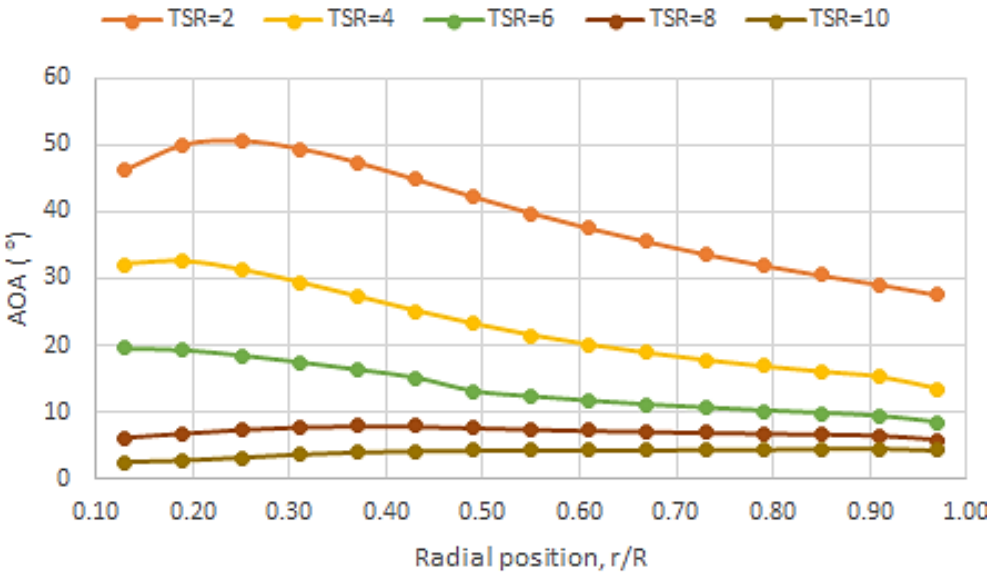

Fig. 5. The graf of AOA against against radial positions of the blade for several TSR

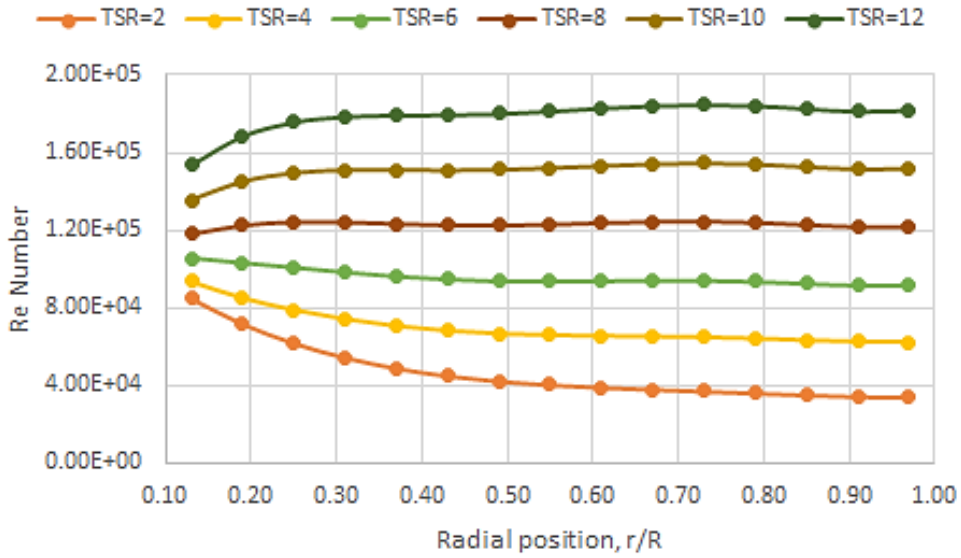

Fig. 6. The graf of Re against against radial positions of the blade for several TSR

3.2 The Aerodynamic Performances using the Extended BEMT

Here, the aerodynamic performance parameters of P, C_P and F_a are discussed with respect to BEMT models considering the tip loss factor, the correction to the high induction factor and the wide ranges of AOA.

The plot of power coefficient against TSR for various models are given in Figure 7. All models show the same pattern of having maximum values at a certain TSR at certain values of TSR as found by other researchers [11, 12]. Again, it can be seen the plot for the BEMT model without the tip loss effect, having higher C_L gives a high maximum value of $C_P = 46.7\%$ at TSR=9. By adding the tip loss factor, the maximum C_P is reduced to 40.8% at TSR of 8. However, the model of Glauert and Wilson-Walker, considering the adjustment made on each axial induction factor, a have increased the C_P to 44.2 at TSR=9 and 46.6 at TSR=10, respectively. It can be seen that different models give different not only the highest C_P but also the peak TSR when this happens. Noted also that at low TSR up until TSR=5, all model give the same plot.

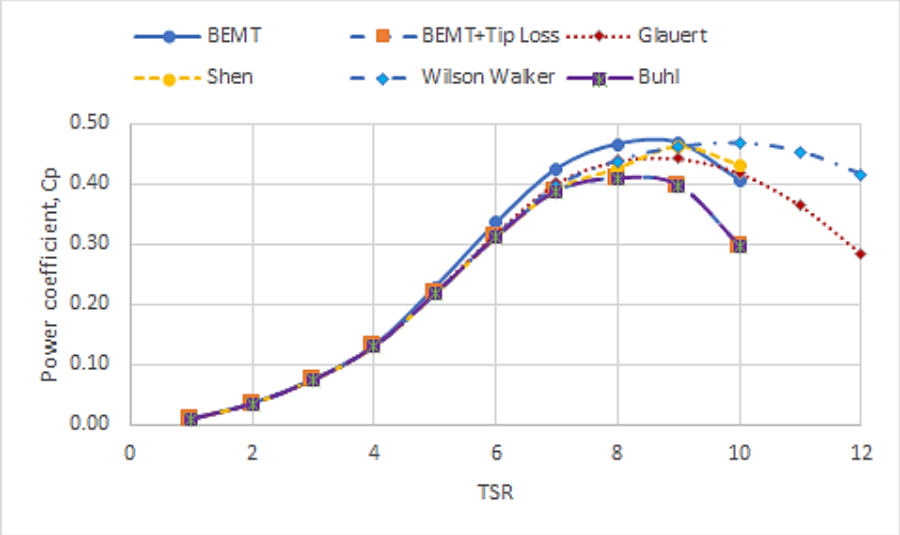

Fig. 7. The power coefficient, C_p against the TSR

Similar plots to C_p vs TSR can be seen in the plot of power vs TSR in Figure 8 where all plots follow the typical plots of power vs TSR where the plot shows maximum values of power at a value of TSR. All models start with the same curve but above TSR=6, the plots starts to split into different curves where the BEMT model give the highest power.

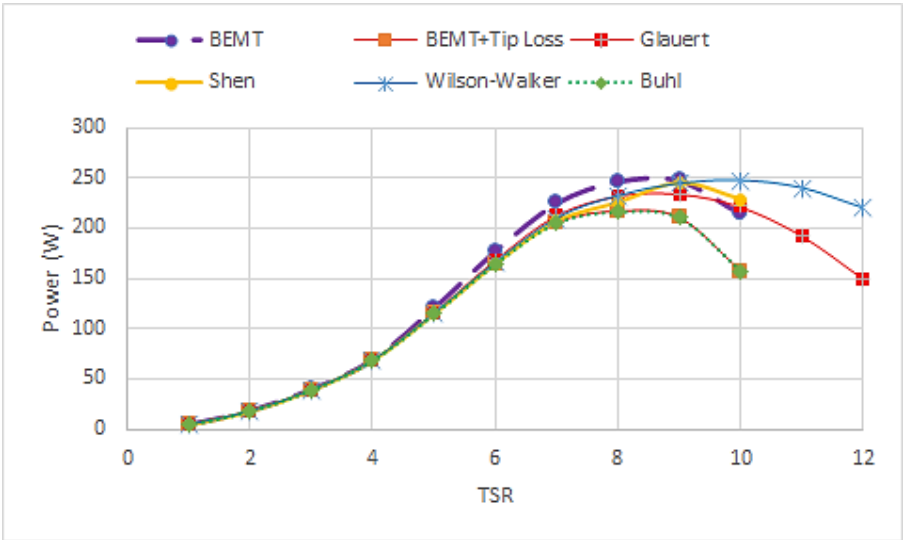

Fig. 8. The power against the TSR

The plots thrust vs TSR for all models considered here can be seen in Figure 9. All models follow the same path until TSR=8 where the plot for each model split. As in the previous plot for aerodynamic performances, the plot for Shen overlaps with the plot for Buhl. Upon the a correction, the Glauert and Wilson-Walker model give the highest thrust. Table 4 shows the peak power along with their TSR, λ_{cr} for each models.

Table 4
The difference between a of 4 different correction models

Model	BEMT	BEMT+ Tip Loss	Gluert	Shen	Wilson-Walker	Buhl
Power, P	247.67	216.38	234.12	245.05	0.201	216.38
TSR, λ_{cr}	9.00	8.00	9.00	9.00	139.2857	8.00

Figure 9 gives the variation of the thrust, F_a for changes of TSR. While all models give the same plot of for TSR of about 8, the curve for each model varies at points following that TSR. The curves can be seen to have no maximum points the BEMT curve are almost the same as the Glauert and the Wilson-Walker plots of up to TSR=9. Noted also that the Buhl's and BEMT models provide similar curves for the power coefficient, power and thrust curves.

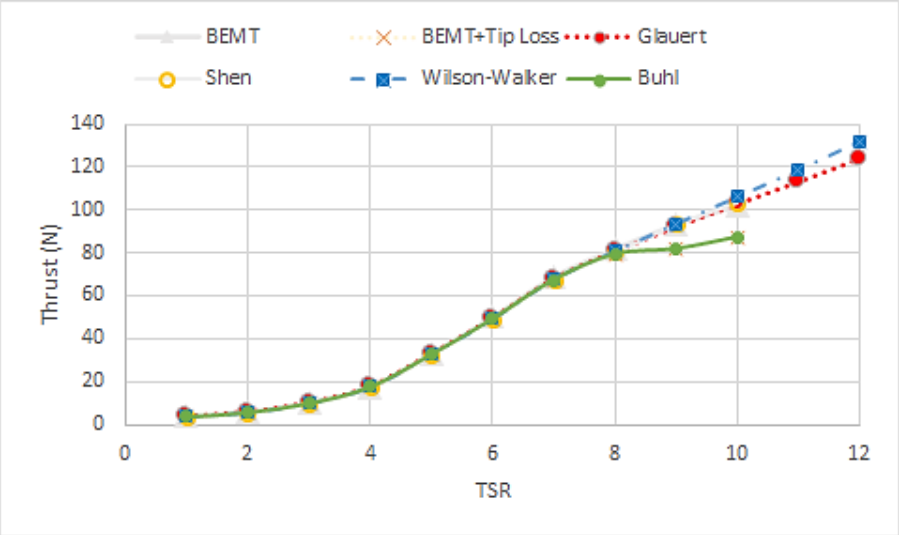

Fig. 9. Thrust, F_a against the TSR

4. Conclusions

The BEMT method has been a popular method in analyzing the aerodynamic performances of wind turbines. However, there are errors to be corrected in the original BEMT equations including in the three areas considered in this study: the tip loss, the low thrust at high axial induction factor and the post-stall region with high angle of attacks. The impact of the tip loss factor especially at the tip region has been discussed. A total of 5 models has been used to compare with the aerodynamic performances of the original (nonextended) BEMT model. The effect of infinite number of blades can be seen here to change the a especially at the tip of the blade and as a result increases the C_L and overpredicts the overall power coefficient and power of the wind turbine.

Acknowledgement

The authors acknowledge the support by the Faculty of Malaysia-Japan Institute of Technology, Universiti Teknologi Malaysia, Kuala Lumpur for providing the UTMER Scheme grant "Q.K.130000.2656.18J24".

References

[1] Khattak, Muhammad Adil, Mohammad Azfar Haziq Ayoub, Muhammad Ariff Fadhlillah Abdul Manaf, Mohd Faidhi Mahru, Mohd Ridwan Mohd Juhari, Mira Idora Mustaffa, and Suhail Kazi. "Global energy security and European Union: A review." *Journal of Advanced Research in Applied Sciences and Engineering Technology* 11, no. 1 (2018): 64-81.

[2] Yusof, Zarina, Zainudin A. Rasid, Mohamad Zaki Hassan, S. M. Sapuan, Shamsul Sarip, Hafizal Yahaya, and Fitri Yakub. "The parametric instability improvement of fully anisotropic composite plates with embedded shape memory alloy." *Advanced Composites Letters* 29 (2020): 2633366X19899405. https://doi.org/10.1177/2633366X19899405

[3] Wahab, AM Abdul, A. Nuh, Z. A. Rasid, A. Abu, Z. Tanasta, M. Z. Hassan, and J. Mahmud. "Tensile behaviours of single-walled carbon nanotubes: Dehnungsverhalten einwandiger Kohlenstoffnanoröhren." *Materialwissenschaft und Werkstofftechnik* 49, no. 4 (2018): 467-471. https://doi.org/10.1002/mawe.201700273
[4] Roslan, S. A. H., Z. Yusof, Z. A. Rasid, M. H. Yahaya, M. Z. Hassan, and J. Mahmud. "Dynamic instability response of smart composite material." *Materialwissenschaft und Werkstofftechnik* 50, no. 3 (2019): 302-310. https://doi.org/10.1002/mawe.201800213
[5] Keong, Chen Wong, and Yusri Yusof. "A Design of New Product Database System for Supporting Step-Compliant Total Integration Applications." *Journal of Advanced Research in Applied Sciences and Engineering Technology* 18, no. 1 (2020): 1-13. https://doi.org/10.37934/araset.18.1.113
[6] Reaches, W.P.C., *546 GW, 60 GW added in 2017.* World Wind Energy Association: Bonn, Germany, 2018.
[7] Lindenberg, S., *20% Wind Energy By 2030: Increasing Wind Energy¿ s Contribution to US Electricity Supply*. 2009: Diane Publishing.
[8] de Freitas Pinto, Ricardo Luiz Utsch, and Bruna Patrícia Furtado Gonçalves. "A revised theoretical analysis of aerodynamic optimization of horizontal-axis wind turbines based on BEM theory." *Renewable Energy* 105 (2017): 625-636. https://doi.org/10.1016/j.renene.2016.12.076
[9] Khattak, M. A., NS Mohd Ali, NH Zainal Abidin, N. S. Azhar, and M. H. Omar. "Common Type of Turbines in Power Plant: A Review." *Journal of Advanced Research in Applied Sciences and Engineering Technology* 3, no. 1 (2016): 77-100.
[10] Venkatramakrishnan, Sri Ragunath, Jitendra K. Pandey, Amit Kumar Mondal, and Ashish Karn. "Low Speed Wind Turbines for Power Generation: A Review." *Journal of Advanced Research in Fluid Mechanics and Thermal Sciences* 67, no. 1 (2020): 146-169.
[11] Oliveira, Hércules Araújo, Luiz Antonio de Souza Ribeiro, Jerson Rogério Pinheiro Vaz, Osvaldo Ronald Saavedra, and José Gomes de Matos. "Comparative study of different correction methods to analyze wind turbine performance." In *2019 IEEE 15th Brazilian Power Electronics Conference and 5th IEEE Southern Power Electronics Conference (COBEP/SPEC)*, pp. 1-6. IEEE, 2019. https://doi.org/10.1109/COBEP/SPEC44138.2019.9065754
[12] Echjijem, Imane, and Abdelouahed Djebli. "Effects of blade design linearization on aerodynamic performance of horizontal axis wind turbine." *International Review of Applied Sciences and Engineering* (2022). https://doi.org/10.1556/1848.2022.00439
[13] Lanzafame, R., and M. Messina. "Design and performance of a double-pitch wind turbine with non-twisted blades." *Renewable Energy* 34, no. 5 (2009): 1413-1420. https://doi.org/10.1016/j.renene.2008.09.004
[14] Roslan, Siti Amni Husna, and Ahmad Kamal Arifin Mohd Ehsan. "The Aerodynamic Performance of the Small-Scale Wind Turbine Blade with NACA0012 Airfoil." *CFD Letters* 14, no. 10 (2022): 87-98. https://doi.org/10.37934/cfdl.14.10.8798
[15] Damirez, V., and G. Augusto. "Power output and power coefficient calculations of a small HAWT with tubercles using Blade Element Momentum Theory." In *IOP Conference Series: Materials Science and Engineering*, vol. 1109, no. 1, p. 012050. IOP Publishing, 2021. https://doi.org/10.1088/1757-899X/1109/1/012050
[16] Anderson, M. B., D. J. Milborrow, and J. N. Ross. "Performance and wake measurements on a 3 m diameter horizontal axis wind turbine. Comparison of theory, wind tunnel and field test data." In *Int. Symp. Wind Energy Syst., Proc.;(United Kingdom)*, vol. 2. 1982.
[17] Çetin, N. S., M. A. Yurdusev, R. Ata, and A. Özdamar. "Assessment of optimum tip speed ratio of wind turbines." *Mathematical and Computational Applications* 10, no. 1 (2005): 147-154. https://doi.org/10.3390/mca10010147
[18] Alaskari, Mustafa, Oday Abdullah, and Mahir H. Majeed. "Analysis of wind turbine using QBlade software." In *IOP conference series: materials science and engineering*, vol. 518, no. 3, p. 032020. IOP Publishing, 2019. https://doi.org/10.1088/1757-899X/518/3/032020
[19] Ighodaro, Osarobo, and David Akhihiero. "Modeling and performance analysis of a small horizontal axis wind turbine." *Journal of Energy Resources Technology* 143, no. 3 (2021). https://doi.org/10.1115/1.4047972
[20] Wood, David. *Small wind turbines*. Springer Berlin Heidelberg, 2011. https://doi.org/10.1007/978-1-84996-175-2
[21] Lanzafame, R. and, and M. Messina. "Fluid dynamics wind turbine design: Critical analysis, optimization and application of BEM theory." *Renewable energy* 32, no. 14 (2007): 2291-2305. https://doi.org/10.1016/j.renene.2006.12.010
[22] Shen, Wen Zhong, Robert Mikkelsen, Jens Nørkær Sørensen, and Christian Bak. "Tip loss corrections for wind turbine computations." *Wind Energy: An International Journal for Progress and Applications in Wind Power Conversion Technology* 8, no. 4 (2005): 457-475. https://doi.org/10.1002/we.153
[23] Buhl Jr, Marshall L. *New empirical relationship between thrust coefficient and induction factor for the turbulent windmill state*. No. NREL/TP-500-36834. National Renewable Energy Lab.(NREL), Golden, CO (United States), 2005. https://doi.org/10.2172/15016819

[24] Vaz, Jerson Rogério Pinheiro, João Tavares Pinho, and André Luiz Amarante Mesquita. "An extension of BEM method applied to horizontal-axis wind turbine design." *Renewable Energy* 36, no. 6 (2011): 1734-1740. https://doi.org/10.1016/j.renene.2010.11.018
[25] Viterna, Larry A., and Robert D. Corrigan. "Fixed pitch rotor performance of large horizontal axis wind turbines." *Large Horizontal-Axis Wind Turbines* (1982).
[26] Vesel Jr, Richard W. "Aero-structural optimization of a 5 MW wind turbine rotor." PhD diss., The Ohio State University, 2012.
[27] Hassanzadeh, Arash, Armin Hassanzadeh Hassanabad, and Abdolrahman Dadvand. "Aerodynamic shape optimization and analysis of small wind turbine blades employing the Viterna approach for post-stall region." *Alexandria Engineering Journal* 55, no. 3 (2016): 2035-2043. https://doi.org/10.1016/j.aej.2016.07.008
[28] Wood, David. *Small wind turbines*. Springer Berlin Heidelberg, 2011. https://doi.org/10.1007/978-1-84996-175-2